Journal of The Electrochemical Society, **148** (8) G411-G419 (2001)
0013-4651/2001/148(8)/G411/9/$7.00 © The Electrochemical Society, Inc.

Silicon Epitaxial Layer Lifetime Characterization

J. E. Park,[a,*] D. K. Schroder,[a,] S. E. Tan,[a] B. D. Choi,[a,*] M. Fletcher,[b] A. Buczkowski,[b,**] and F. Kirscht[b]**

[a]*Department of Electrical Engineering and Center for Solid State Electronics Research, Arizona State University, Tempe, Arizona 85287-5706, USA*
[b]*Mitsubishi America, Salem, Oregon 97303, USA*

Surface photovoltage (SPV) measurements are traditionally carried out under steady-state conditions to determine the minority carrier diffusion length. While this technique is very convenient for bulk wafer defect characterization, especially the detection of iron in boron-doped silicon wafers, it is poorly suited to characterize epitaxial layers that are typically much thinner than the minority carrier diffusion length. We have developed the theory for frequency-dependent SPV measurements and have verified this theory with experimental data. We consider the various recombination/generation components in the semiconductor and determine the dependence on photon flux density, optical absorption coefficient, doping density, recombination lifetime, and temperature. Epitaxial layers are usually measured with techniques that are sensitive to generation parameters confined to the reverse-biased space-charge region (scr). We show that optical excitation can be used for scr confined recombination measurements, but the resultant lifetime is an effective lifetime incorporating both scr and surface recombination, heavily influenced by surface recombination.
 [DOI: 10.1149/1.1380257]

Manuscript submitted December 7, 2000; revised manuscript received April 4, 2001. Available electronically July 3, 2001.

It is difficult to characterize epitaxial layers through recombination lifetime or minority carrier diffusion length measurements because the layers are usually much thinner than the minority carrier diffusion length. We discuss the various difficulties with the aid of Fig. 1. In Fig. 1a we show a p-type epitaxial layer on a p^+ substrate, with optical excitation as used for conventional recombination lifetime measurements. Electron-hole pairs (ehps) are generated either in the epitaxial layer and the substrate with penetrating light or in the epi layer alone with short wavelength light. Excess carriers recombine at the surface, in the epi layer itself, at the epi/substrate interface, and in the substrate. The resultant lifetimes or diffusion lengths are effective values strongly influenced by recombination at the surface and at the epi/substrate interface. Even if the surface is oxidized to reduce surface recombination, the Si/SiO_2 interface can still be a strong contributor to the effective lifetime.

Let us consider the excess carriers to be reasonably well confined to the epi layer due to the minority carrier potential barrier at the epi/substrate interface. If the epi layer lifetime is τ_{epi}, the surface lifetime is τ_{s1}, and the epi/substrate interface lifetime is τ_{s2}, the effective lifetime is[1]

$$\frac{1}{\tau_{eff}} = \frac{1}{\tau_{epi}} + \frac{1}{\tau_{s1}} + \frac{1}{\tau_{s2}} \approx \frac{1}{\tau_{epi}} + \frac{2s_{r1}}{t_{epi}} + \frac{2s_{r2}}{t_{epi}} \qquad [1]$$

using $\tau_s \approx t_{epi}/2s_r$, where t_{epi} is the epitaxial layer thickness and s_r the surface or interface recombination velocity. The substrate lifetime is not included in Eq. 1, because the excess carriers are largely confined to the epi layer.

To illustrate the effect of surface/interface recombination on the recombination properties, we have plotted τ_{eff} *vs.* epi layer thickness as a function of τ_{epi}, s_{r1}, and s_{r2} in Fig. 2 for $s_{r1} = s_{r2} = 1$ and 100 cm/s. For $t_{epi} < 4s_r\tau_{epi}$, the effective lifetime is dominated by interfacial recombination and for $t_{epi} > 4s_r\tau_{epi}$ by epitaxial layer recombination. For a typical epi layer thicknesses of 10^{-4} to 10^{-3} cm, the effective lifetime is largely dominated by interfacial recombination for lifetimes of 10 μs or higher. The lifetime of high quality bulk Si wafers is typically in the 1-10 ms range. Epitaxial layers are likely to be slightly worse with lifetimes in the 100 μs range due to slightly higher metallic contamination. Figure 2 shows that in order to be able to say anything about the epi layer lifetime, the surface recombination velocity has to be very low. Such low s_r can be achieved through effective chemical surface passivation or by driving the surface into accumulation with corona charge.[2]

Hara *et al.* used microwave photoconductance decay with 902 nm light (absorption depth about 25 μm) to characterize 30 μm thick epitaxial layers on lightly doped substrates.[3] For bare wafers, they measured an effective recombination lifetime of 8 μs. Passivating the epi surface with an iodine/methanol solution reduced the surface recombination velocity to about 10 cm/s and increased the lifetime to 120 μs. Etching the epi layer gave a substrate lifetime of 153 μs. After correcting for the substrate lifetime, they calculated the epi layer lifetime to be 450 μs. Changing the light source to 520 nm (absorption depth about 1.1 μm) did not help the measurement. They found the epi lifetime to be about the same as the substrate lifetime (around 58 μs).

Ogita *et al.* characterized p/p^+ and n/n^+ samples using 337.1 nm ultraviolet light (N_2 laser) and high frequency (100 GHz) microwaves.[4] The excess carriers generated by UV light with absorption depth of 20 nm, are confined to the near-surface region. They found that by depositing negative ions on the surface to reduce surface recombination, the effective lifetime increased from 0.76 to 5 μs. Consequently, they claimed $\tau_{epi} \geqslant 5$ μs and the interfacial recombination velocity to be ≤320 to 380 cm/s. Hence, even under these measurement conditions, surface and interface recombination are important. Pavelka and Batari used corona charge and found the effective lifetime on an 8 μm thick epi layer as high as 50 μs.[2] From Fig. 2, this would indicate a true epi lifetime on the order of 100 μs or so.

Surface photovoltage measurements with penetrating light have the problem that ehps are generated in both regions, but the minority carrier diffusion length, L_n, in the heavily doped substrate is usually much lower than that in the epi layer. Hence, the measurements typically yield t_{epi} rather than L_n.

Due to these difficulties, space-charge region (scr) measurements have usually been made with electron-hole pair generation/recombination largely confined to the space charge region (scr) illustrated in Fig. 1b. Such methods include measuring the leakage current of reverse-biased p-n junctions,[5] the recovery time of pulsed metal oxide semiconductor capacitors,[6] or the frequency dependence of an scr-dependent parameter.[7-8] The emergence of commercially available charge-based semiconductor characterization tools has opened up the possibility of making such lifetime measurements on oxidized Si wafers without having to fabricate devices.[9]

The current of a reverse-biased junction is given by

* Electrochemical Society Student Member.
** Electrochemical Society Active Member.

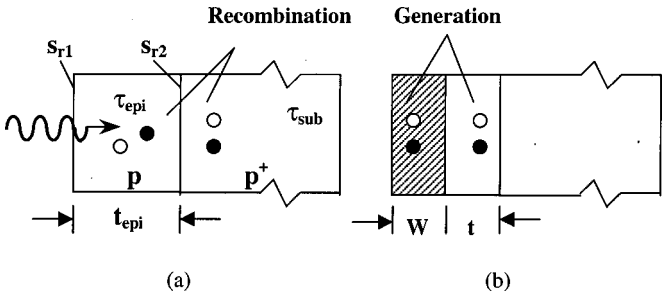

Figure 1. Epitaxial layer lifetime characterization difficulties: (a) conventional recombination lifetime, (b) scr lifetime measurements.

$$J = \frac{qn_i W}{\tau_g} + \frac{qn_i^2 D_n}{N_{A,epi} L_n} \quad [2]$$

where q is the electron charge, W the scr width, n_i the intrinsic carrier density, τ_g the generation lifetime, D_n the diffusion coefficient, and $N_{A,epi}$ the epi layer doping density. The current density in the first term in Eq. 2 is due to (scr) generation, the second term due to quasi-neutral region (qnr) generation. It is important during these measurements for scr generation to dominate. However, qnr generation does contribute at room temperature and becomes more important at elevated temperatures.

For epitaxial layers, one should use an effective diffusion length, $L_{n,eff}$, given by

$$L_{n,eff} = \frac{L_n}{F} \quad [3]$$

where the correction factor F is given by[10]

$$F = \frac{(1 + N_{A,sub}/N_{A,epi})\ \exp(t/L_n) + (1 - N_{A,sub}/N_{A,epi})\ \exp(-t/L_n)}{(1 + N_{A,sub}/N_{A,epi})\ \exp(t/L_n) - (1 - N_{A,sub}/N_{A,epi})\ \exp(-t/L_n)} \quad [4]$$

with t as the undepleted epi layer thickness, indicated on Fig. 1b. $N_{A,sub}$ is the substrate doping density. The correction factor, F, is plotted in Fig. 3. Clearly for long diffusion length and high $N_{A,sub}$, the correction factor becomes substantial making L_{neff} significantly higher than L_n. In spite of the diffusion length uncertainty, scr measurements are effective epi layer characterization techniques.

SCR-based measurements can be augmented with optical excitation and contactless probe detection. Typically, an scr is formed through an appropriate rinse of the sample or through corona charge deposition. Low level light with high absorption coefficient ensures low density electron hole pair generation in the space charge region.[11] The scr electric field serves to separate the ehps. The optically generated carriers lead to a slight forward bias, which in turn, leads to carrier injection into the qnr. Hence, one needs to address scr and qnr recombination and generation. In addition, since carriers are generated near the surface, surface recombination also needs to be taken into account.

We present in this paper the relevant theory, supported by experimental data, of charge-based, light-excited probe measurements of epitaxial layers. We show that for short wavelength light, confining the optically generated carriers largely to the scr, we characterize the near-surface region of the epitaxial layer, by measuring the recombination lifetime in the scr. This lifetime is a combination scr and surface recombination lifetime, but it is dominated by surface recombination.

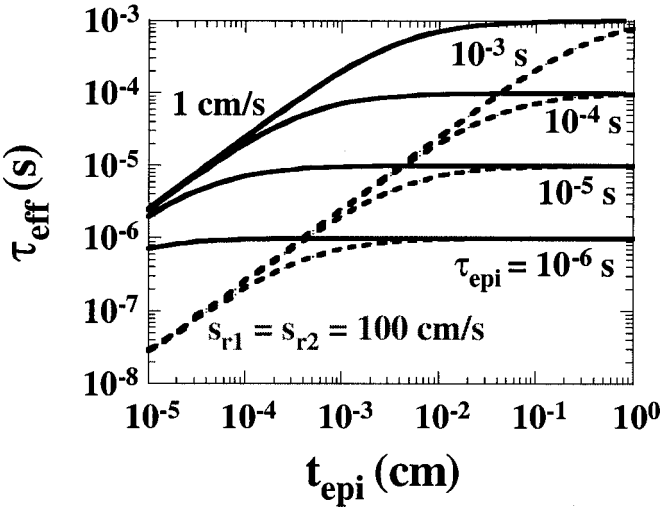

Figure 2. Effective recombination lifetime *vs.* epitaxial layer thickness as a function of epitaxial layer lifetime.

Surface Charging

A crucial component for charge-based measurements is the surface treatment to create the surface scr. Two options are available: treat the surface chemically, or deposit corona charge. During chemical treatment, for n-type silicon, the oxide on the sample surface should be removed and then the sample should be boiled in H_2O_2 or in water for about 15 min and then rinsed in deionized (DI) water.[12] Alternately, one can soak the sample in $KMnO_4$ for 1-2 min and then rinse in DI water. These treatments produce a stable deple-

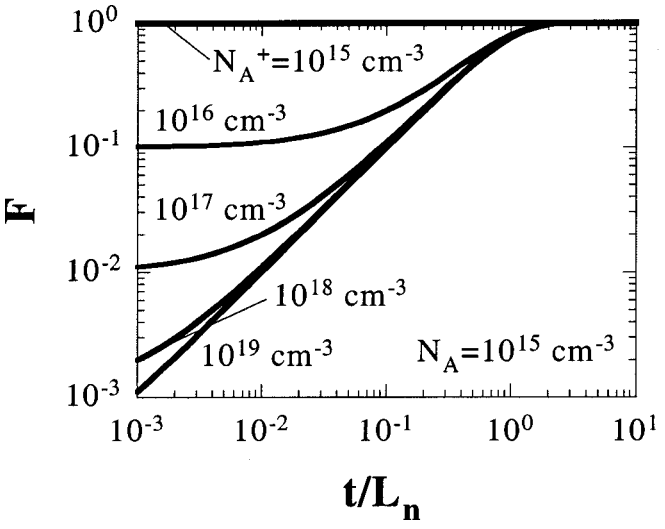

Figure 3. Correction factor F *vs.* t/L_n.

tion surface potential barrier. For p-type silicon, very little treatment is required. In case of very low surface photovoltage (SPV), V_{SPV}, etching in buffered HF followed by a DI water rinse is recommended.

Corona charging consists of depositing ions on a surface at atmospheric pressure through an electric field applied to a source of ions. The corona source consists of a wire, a series of wires, a single point, or multiple points located a few mm or cm above the sample surface.[13] The substrate may be moved during charging or between charging cycles and the sample may be charged uniformly or in well-defined areas through a mask arrangement. A potential of 5,000-10,000 V of either polarity is applied to the corona source. Ions are generated close to the electrode. For a negative source potential, positive ions bombard the source while ambient molecules capture free electrons to form negative ions. For a positive source potential, electrons are attracted to the source and positive ions follow the electric field lines to the substrate. The negative and positive corona ionic species are predominantly CO^{-3} and H_3O^+ (hydrated protons), respectively. The corona source forces a uniform flow of ionized air molecules toward the surface. The very short (approximately 0.1 μm) atmospheric mean free path of the ionized gas ensures collision-dominated ion transport with the molecules retaining very little kinetic energy. Typically a few seconds are required to charge an insulating surface to a saturating potential. The charge is not permanent and can be removed by a water rinse.

During charge-based measurements, charge is deposited on the wafer and its response is measured by one of several techniques. One can drive the corona-oxide-semiconductor (COS) device into deep depletion and measure the recovery response with a contactless probe.[9,14] It is also possible to bias the COS device into depletion or inversion and measure the frequency response by varying the electrical signal applied to the probe or by applying a time-varying optical signal to the device.[7]

To understand surface charge-based measurements, it is helpful to understand contactless probe measurements. Lord Kelvin first proposed the Kelvin probe in 1881.[15] Kronik and Shapira give an excellent explanation of Kelvin probes and their various applications.[16] We will explain its operation with the aid of Fig. 4. Consider a p-type semiconductor with a grounded substrate. A metal probe is placed a distance, d (typically 0.1-1 mm), from the wafer surface. In this discussion, we assume the work functions of the metal and the semiconductor to be identical. With no surface charge on the semiconductor surface, the semiconductor bands are flat, as shown by the dashed energy band diagram in Fig. 4a and the probe potential, also known as the contact potential difference, V_{cpd}, is zero. For positive surface charge, the semiconductor is depleted, as shown by the solid energy band diagram in Fig. 4a.

The electrically floating probe will assume a positive contact potential difference V_{cpd} equal to the surface potential ϕ_s, because no charge is deposited on the electrically floating probe, and hence, there is no electric field between the semiconductor surface and the probe. When the semiconductor is illuminated, the Fermi level splits into two quasi-Fermi levels and both the semiconductor band bending and V_{cpd} are reduced, as illustrated in Fig. 4b. Since we are dealing with optically induced voltages in this paper, we will designate the probe voltage as the surface photovoltage V_{SPV}. Photons, incident on the sample, generate excess carriers within the scr and in the quasi-neutral bulk region. The electrons within the scr and within a distance of approximately the minority carrier diffusion length from the edge of the scr will be collected in the scr and they reduce the surface potential barrier slightly. The barrier lowering is similar to a forward-biased junction and the probe detects the difference of the quasi-Fermi levels. For high level injection, the surface potential vanishes.[17] However, we use low level injection leading to low surface potentials.

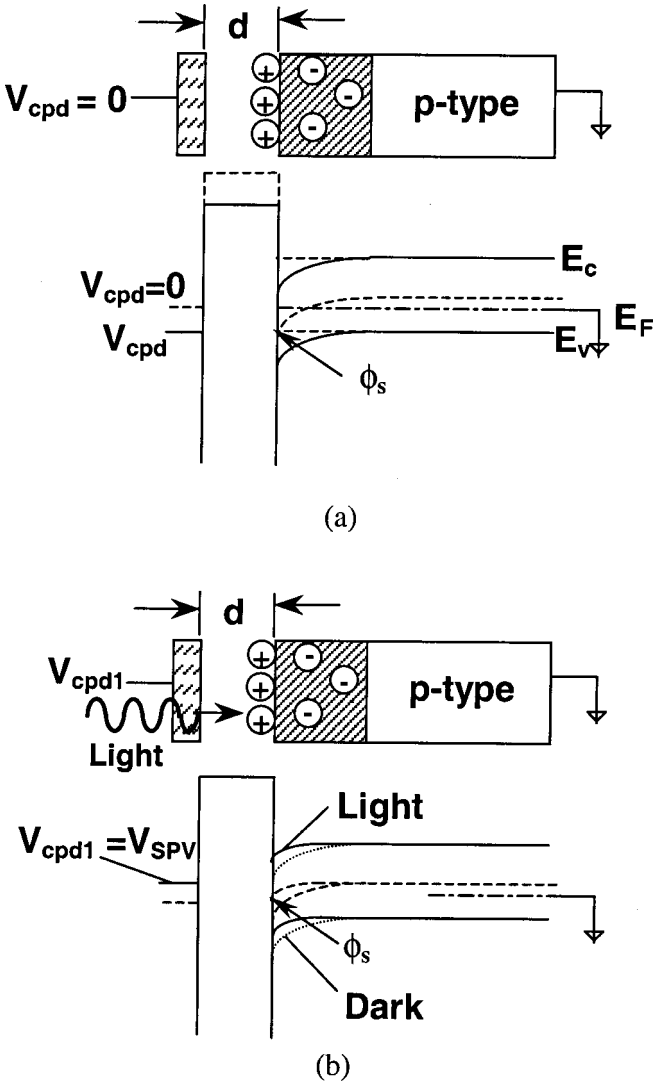

Figure 4. Probe energy band diagram for (a) in the dark without and with surface charge, and (b) with surface charge and optical excitation.

Theory

Consider the sample configuration of Fig. 5. Charge on the surface of the p-type wafer induces a space charge of width W. Incident light generates ehps in the sample and the resulting surface photovoltage is measured. We treat the general case of recombination and generation in both the scr and in the quasi-neutral region. s_r is the surface recombination velocity, $\tau_{r,scr}$ the scr recombination lifetime, L_n the quasi-neutral region minority carrier diffusion length, $\tau_{g,scr}$ the scr generation lifetime, and $\tau_{g,qnr}$ the qnr generation lifetime. With light creating excess carriers, recombination dominates over generation and we neglect the generation components. Furthermore, since it is impossible to separate surface and bulk scr recombination with a simple two-terminal measurement, we combine s_r and $\tau_{r,scr}$ into the effective lifetime, τ_{scr}. This lifetime is also known as the surface lifetime or the surface-dominated lifetime.

We use the equivalent circuit of Fig. 6 to represent the semiconductor under ac light excitation. The monochromatic, ac-modulated light generates the photocurrent I_{ph}. The capacitance, C_{scr} represents the semiconductor surface charge-induced scr and C_{probe} is the probe capacitance, given by

$$C_{scr} = \frac{K_s \varepsilon_o}{W} = \frac{1.04 \times 10^{-12}}{W} = 2.1 \times 10^{-8}$$

$$C_{probe} = \frac{\varepsilon_o}{d} = \frac{8.85 \times 10^{-14}}{d} \approx 8.8 \times 10^{-12} \text{ F/cm}^2 \quad [5]$$

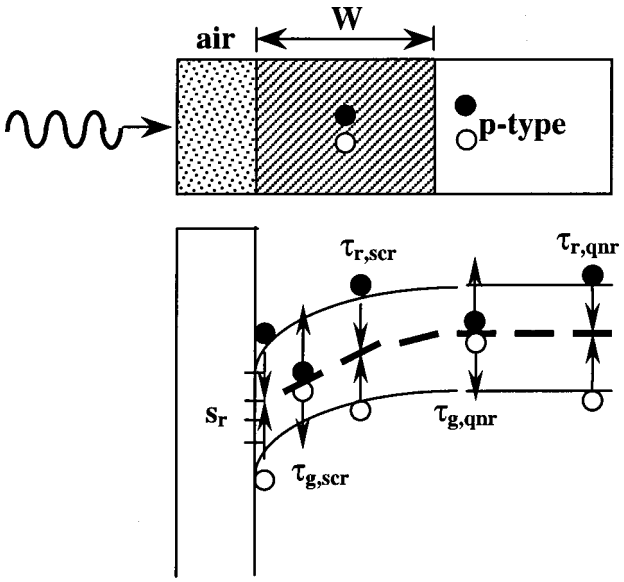

Figure 5. The sample geometry and the conductances (G) due to generation and recombination of excess carriers.

for $W = 0.5\,\mu m$ and $d = 100\,\mu m$. Clearly, $C_{scr} \gg C_{probe}$. The conductances, G, represent the various loss mechanisms in the semiconductor due to carrier recombination as illustrated in Fig. 5. G_{scr} and G_{qnr} represent recombination in the scr and qnr regions. We have also considered generation in both scr and qnr, shown in Fig. 5, and find the generation conductances to be negligible compared to recombination conductances and do not consider them further.

We consider a p-type substrate and concentrate on the behavior of the minority electrons. Optical carrier generation by high absorption coefficient light is largely confined to the scr. These excess carriers recombine in the scr and at the surface, and some are injected into the quasi-neutral region to recombine there. Recombination in the scr leads to the conductance G_{scr}

$$G_{scr} = \frac{J_r}{V_{SPV}} \approx \frac{\dfrac{qn_iW}{\tau_{scr}}\left[\exp\left(\dfrac{qV_{SPV}}{kT}\right) - 1\right]}{V_{SPV}} \approx \frac{q^2n_iW}{\tau_{scr}kT} \qquad [6]$$

where W is the scr width, and τ_{scr} the effective lifetime due to recombination in the scr and at the surface. The scr recombination

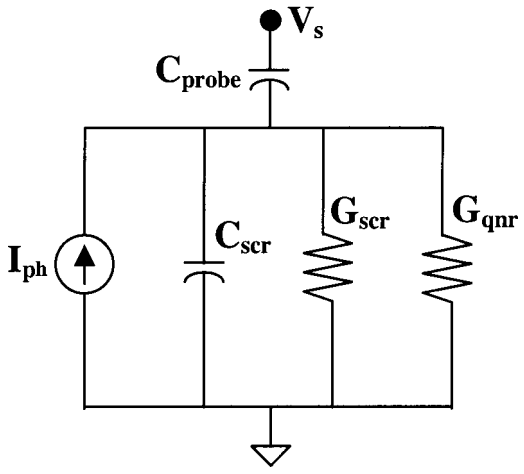

Figure 6. The equivalent circuit of the SPV measurement system.

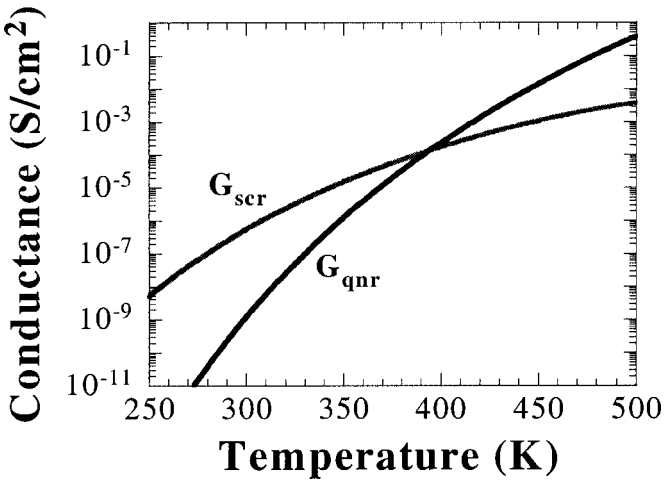

Figure 7. Conductances *vs.* temperature. $\tau_{scr} = 10\ \mu s$, $\tau_r = 10\ \mu s$, $N_A = 10^{15}\ cm^{-3}$.

current density can be expressed in terms of the scr recombination lifetime $\tau_{r,scr}$ and surface recombination velocity s_r, as

$$J_{scr} = qn_i\left(\frac{W}{\tau_{r,scr}} + s_r\right)\left[\exp\left(\frac{qV_{SPV}}{kT}\right) - 1\right] = \frac{qn_iW}{\tau_{scr}}\left[\exp\left(\frac{qV_{SPV}}{kT}\right) - 1\right] \qquad [7]$$

where $\tau_{scr} = \tau_{r,scr}/(1 + s_r\tau_{r,scr}/W)$, *i.e.*, it is a combination of the two recombination parameters.

The qnr recombination conductance (G_{qnr}) due recombination in the quasi-neutral region is given by

$$G_{qnr} = \frac{J_{rqnr}}{V_{SPV}} \approx \frac{\dfrac{qn_i^2D_n}{N_AL_n}\left[\exp\left(\dfrac{qV_{SPV}}{kT}\right) - 1\right]}{V_{SPV}} \approx \frac{q^2n_i^2D_n}{N_AL_nkT} = \frac{q\mu_nn_i^2}{N_AL_n} \qquad [8]$$

where μ_n is the electron mobility, N_A the doping density, and L_n the diffusion length given by $L_n = (D_n\tau_r)^{1/2}$, where τ_r is the recombination lifetime in the quasi-neutral region. We use L_n rather than $L_{n,eff}$ in our analyses with little error since, as we show later, qnr recombination is generally negligible. The conductances are plotted in Fig. 7. The scr recombination conductance, G_{scr}, dominates for $T \leqslant 400$ K for this example. This is similar to the scr or Sah-Noyce-Shockley recombination current dominating in Si p-n junction at low voltages around room temperature.

So far, we have been concerned with dc behavior. However, since we are ultimately interested in ac excitation, the ac behavior of the various lifetimes should be considered. Mathematical analyses of steady-state solutions usually assume all pertinent parameters to have an "exp($j\omega t$)" dependence, with $\omega = 2\pi f$ the radial frequency. A consequence of this modification is that the diffusion length and the lifetime become time-varying functions, defined by[18]

$$L_n = \frac{L_{no}}{\sqrt{1 + j\omega t}} \quad \tau = \frac{\tau_o}{1 + j\omega t} \qquad [9]$$

where L_{no} and τ_o are the dc values.

To determine the frequency-dependent nature of the equivalent circuit, we consider the circuit in Fig. 6. The photocurrent flows

primarily through C_{scr}, G_{scr}, and G_{qnr}. The current through C_{probe} can be neglected, because the probe terminal is connected to a high impedance voltmeter and C_{probe} is a very small capacitance leading to a high impedance. The impedance is given by

$$Z = \frac{1}{G_{tot} + j\omega C_{scr}} \quad [10]$$

where

$$G_{tot} = G_{scr} + G_{qnr} \quad C_{scr} = K_s\varepsilon_o/W \quad [11]$$

The phase angle, θ, is given by

$$\theta = \tan^{-1}(X/R) \quad [12]$$

where X is the reactance and R the resistance, related to the impedance by

$$Z = \sqrt{R^2 + X^2} \quad [13]$$

With G_{scr} dominating in the relevant temperature range, according to Fig. 7, Eq. 10 becomes

$$G_{tot} \approx G_{scr} = \frac{q^2 n_i W}{\tau_{scr} kT} = \frac{1}{\eta\tau_{scr}} \quad [14]$$

with $\tau_{scr} = \tau_{scro}/(1 + j\omega\tau_{scro})$.

The impedance and phase become

$$Z \approx \frac{G_{scr}^{-1}}{1 + j\omega C_{scr}/G_{scr}} = \frac{kT\tau_{scro}}{q^2 n_i W(1 + j\omega/\omega_c)} \quad [15]$$

$$\theta = \tan^{-1}(\omega/\omega_c) \quad [16]$$

The corner frequency, ω_c, is

$$\omega_c = \frac{1}{\tau_{scro}\left(1 + \frac{kTC_{scr}}{q^2 n_i W}\right)} = \frac{1}{\tau_{scro}\left(1 + \frac{kTK_s\varepsilon_o}{q^2 n_i W^2}\right)} = \frac{1}{\tau_{scro}\left(1 + \frac{kTN_A}{2qn_i\phi_s}\right)} \quad [17]$$

where ϕ_s is the surface potential. The corner frequency depends on the low frequency scr recombination lifetime, τ_{scro}, the surface potential ϕ_s, the doping density N_A, and n_i.

The electrode measures the barrier lowering or the V_{SPV} shown in Fig. 4. The photocurrent in the scr is[1]

$$J_{scr} = q\Phi(1 - R)[1 - \exp(-\alpha W)] \quad [18a]$$

where Φ is the photon flux density, R the reflectivity, α the absorption coefficient, and W the scr width. The photocurrent in the uniformly doped quasi-neutral region of thickness d with diffusion length L_n, is

$$J_{qnr} = \frac{q\Phi(1 - R)\alpha L_n \exp(-\alpha W)}{\alpha^2 L_n^2 - 1}\left[\alpha L_n - \frac{k_n\cosh(\phi) + \sinh(\phi) - (k_n - \alpha L_n)\exp(-\alpha d)}{\cosh(\phi) + k_n\sinh(\phi)}\right] \quad [18b]$$

giving the total photocurrent as

$$J_{ph} = J_{scr} + J_{qnr} \quad [19]$$

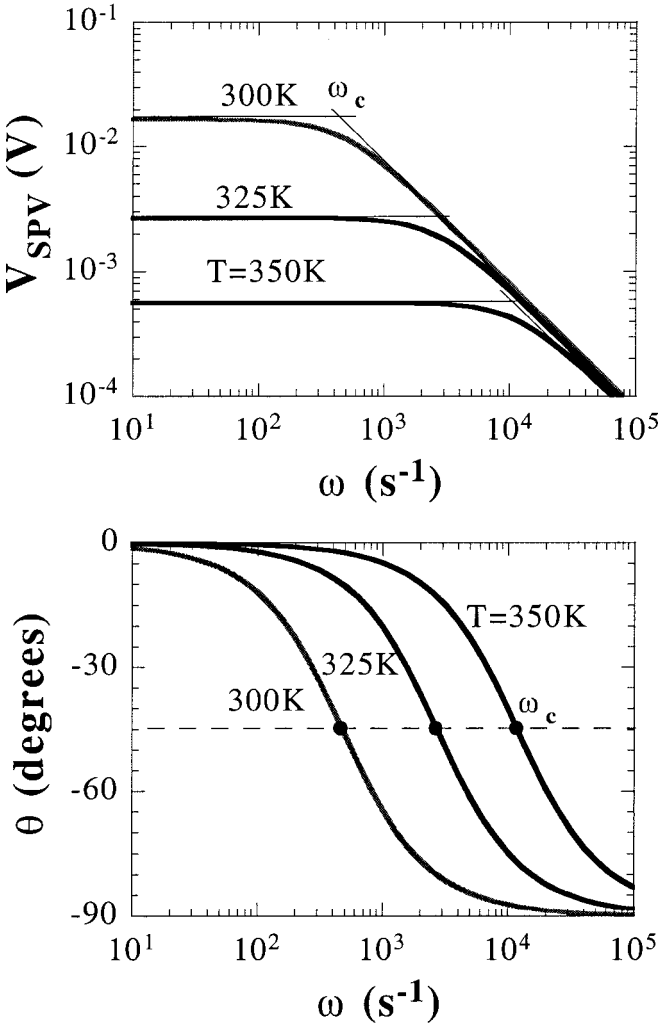

Figure 8. V_{SPV} and θ *vs.* ω as a function of temperature for $\Phi = 10^{12}$ cm^{-2} s^{-1}, $R = 0.3$, $\alpha = 2 \times 10^4$ cm^{-1}, $W = 0.8$ μm, $\tau_{scro} = 10^{-6}$ s, $\tau_{ro} = 10^{-5}$ s, $N_{A,epi} = 10^{15}$ cm^{-3}.

where $k_n = s_n L_n/D_n$ and $\phi = t/L_n$. For epitaxial wafers with two different doping densities and very likely two different diffusion lengths, the J_{qnr} expression becomes more complicated. For light with high absorption coefficient, appropriate for our experimental conditions, J_{scr} dominates over J_{qnr} and $J_{ph} \approx J_{scr}$. J_{qnr} is only about 1% or less of the total photocurrent in our experiments.

The surface photovoltage is

$$V_{SPV} = J_{ph}Z \quad [20]$$

The surface photovoltage and phase angle θ are plotted *vs.* radial frequency as a function of temperature in Fig. 8. For our measurements the excitation wavelength has a wavelength of 400 nm and an absorption coefficient of 2×10^4 cm^{-1}, leading to an absorption depth 1/α of 0.5 μm with most of the light absorbed in the scr.

The lifetime is obtained from the corner frequency expression of Eq. 17, with the corner frequency, ω_c, obtained from either the surface photovoltage or from the 45° angle of the phase plot. To check whether the approximation of Eq. 15 is valid, we have plotted in Fig. 9 ω_c calculated with Eq. 17 (solid line) and with points taken from $V_{SPV} - \omega$ plots (points) using the full conductance expression in Eq. 11. This figure clearly shows that the approximation is excellent, verifying that scr recombination is indeed the dominant mechanism. According to Eq. 17, the temperature dependence of ω_c is

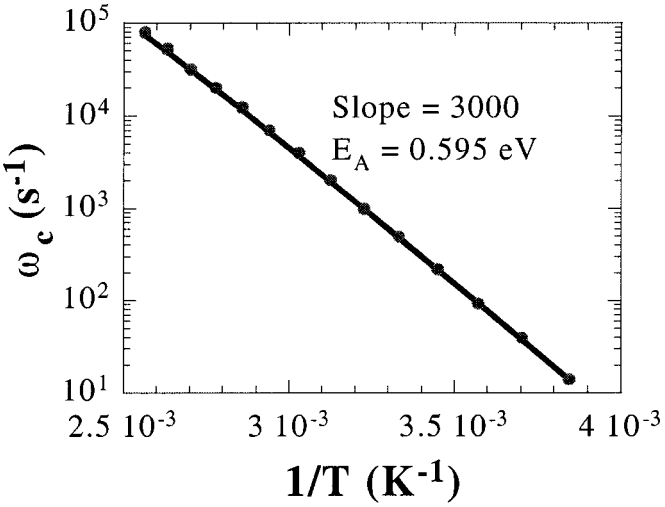

Figure 9. Corner frequency *vs.* $1/T$ for $\Phi = 10^{12}$ cm^{-2} s^{-1}, $R = 0.3$, $\alpha = 2 \times 10^4$ cm^{-1}, $W = 0.8$ μm, $\tau_{scro} = 10^{-6}$ s, $\tau_{ro} = 10^{-5}$ s, $N_A = 10^{15}$ cm^{-3}. Line: approximation, points: full expression.

chiefly determined by n_i. The semilog plot of Fig. 9 should, therefore, give the activation energy E_A of n_i, which it does.

To understand the effect of optical excitation, we consider the device impedance and the way that impedance is modified by light. Impedances are most commonly measured with electrical excitation, where the device is excited with a current and the resulting voltage is measured. To understand the measurement with optical excitation, we simplify the circuit of Fig. 6 to that in Fig. 10, where G represents the conductances from Fig. 6 and G_{ph} represents the photoconductance. The impedance of the circuit in Fig. 10 is

$$Z = \frac{1}{G + G_{ph} + j\omega C_{scr}} \qquad [21]$$

The conductances are defined as

$$G = \frac{J}{V} = \frac{q\int Rdx}{V} \quad G_{ph} = \frac{J_{ph}}{V} \qquad [22]$$

where R is the recombination/generation rate. For low level excitation, the photocurrent should be low compared to the thermally generated current, *i.e.*

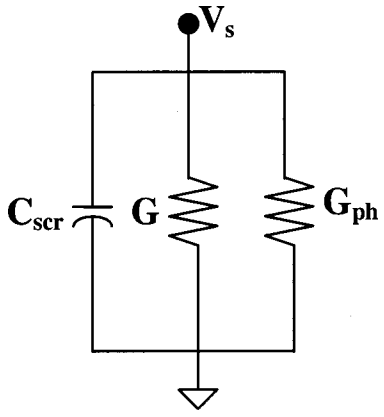

Figure 10. Simplified equivalent circuit.

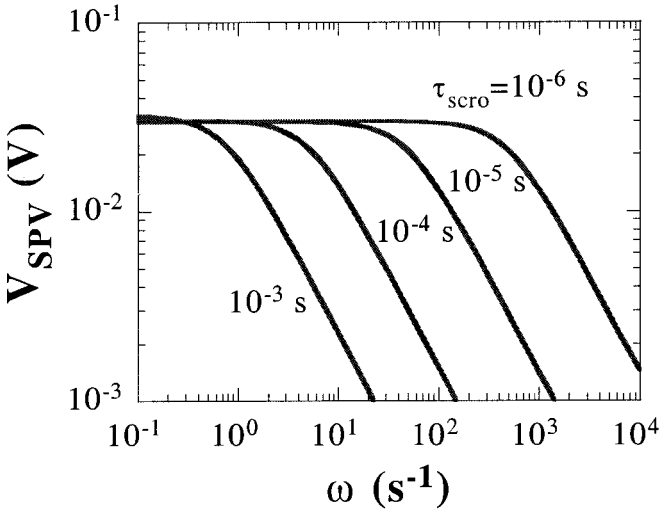

(a)

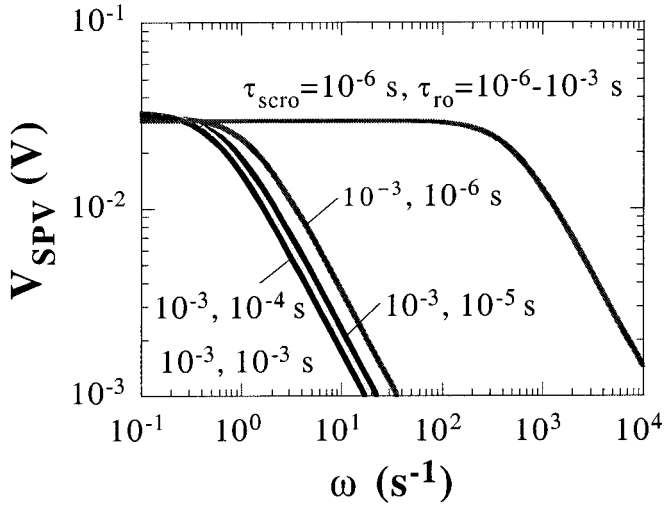

(b)

Figure 11. V_{SPV} *vs.* ω as a function of scr recombination lifetime for $\alpha = 2 \times 10^4$ cm^{-1}, $R = 0.3$, $W = 0.8$ μm, $N_A = 10^{15}$ cm^{-3}, $T = 300$ K. (a) $\tau_{ro} = 10^{-5}$ s, (b) τ_{ro} varies from 10^{-6} to 10^{-3} s. The curves are normalized to $V_{SPV} = 0.03$ V.

$$J_{ph} = q\eta\Phi < q\int Rdx \qquad [23]$$

where η is the quantum efficiency. Equation 23 leads to

$$\Phi < \frac{\int Rdx}{\eta} = \frac{qn_iWV_s}{kT\eta\tau_{scr}} \approx \frac{n_iW}{\eta\tau_{scr}} \qquad [24]$$

for scr recombination to dominate, as shown earlier. The approximation holds for $V_{SPV} \approx kT/q$, as is typical for surface photovoltage measurements. Using $n_i = 10^{10}$ cm^{-3}, $W = 10^{-4}$ cm, $\tau_{scr} = 10^{-6}$ s, and $\eta = 0.5$, leads to $\Phi < 2 \times 10^{12}$ photons/cm^2-s. This restriction is relaxed at elevated temperatures. For example, at $T = 100$°C, $n_i = 1.4 \times 10^{12}$ cm^{-3}, leading to $\Phi < 3 \times 10^{14}$ photons/cm^2-s.

Before considering experimental data, we examine the effect of various parameters on $V_{SPV} - \omega$ plots.

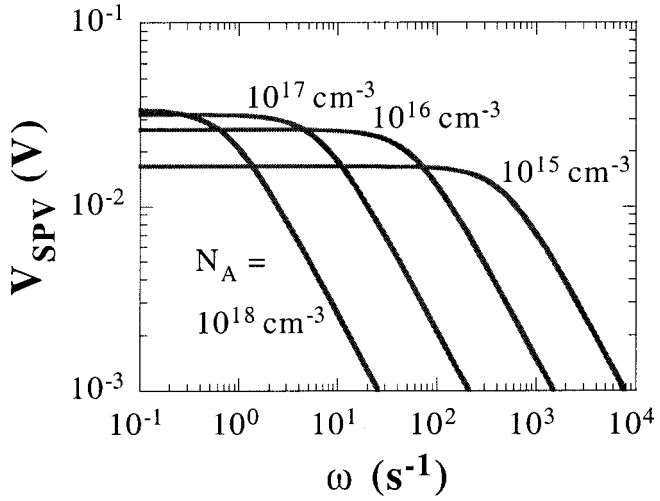

Figure 12. Surface photovoltage *vs.* frequency as a function of epi doping concentration. $\tau_{scro} = 1$ μs, $\tau_{ro} = 10$ μs, $\Phi = 10^{12}$/ cm^{2}s, $T = 300$ K.

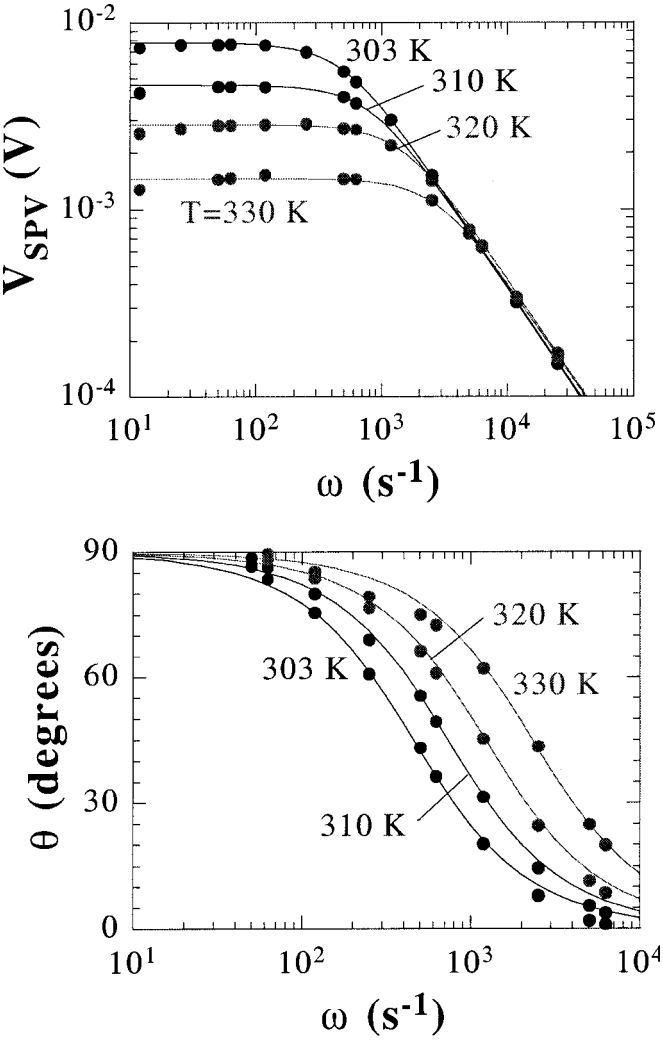

Figure 13. Surface photovoltage and phase *vs.* frequency as a function of temperature. Experiment: $t_{epi} = 10$ μm, $N_{A,epi} = 10^{15}$ cm^{-3}, $N_{A,sub} = 10^{18}$ cm^{-3}. Theory: $\alpha = 2 \times 10^4$ cm^{-1}, $W = 0.8$ μm, $\tau_{ro} = 10^{-5}$ s, $N_{A,epi} = 10^{15}$ cm^{-3}. Points: experiment; lines: theory.

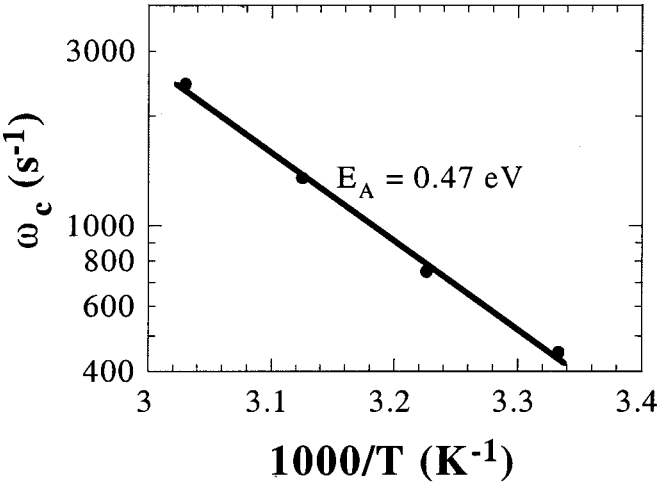

Figure 14. Corner frequency *vs.* inverse temperature. $t_{epi} = 10$ μm, $N_{A,epi} = 10^{15}$ cm^{-3}, $N_{A,sub} = 10^{18}$ cm^{-3}.

Effect of lifetimes.—The surface photovoltage obviously depends on the various lifetimes, but which lifetime has the major effect on the surface photovoltage? To answer that question, we have calculated the effects of scr and qnr lifetimes and show the results in Fig. 11 with the lifetime parameter being the scr recombination lifetime τ_{scro}. In Fig. 11a, only τ_{scro} is varied. Varying the qnr lifetime τ_{ro} from 10^{-6} to 10^{-3} s has almost no effect for $\tau_{scro} = 10^{-6}$ s, as shown in Fig. 11b, but does have a small effect for $\tau_{scro} = 10^{-3}$ s. The message here is clearly that scr recombination is the dominant mechanism. τ_{scro} is related to the corner frequency through Eq. 17 as

$$\tau_{scro} = \frac{1}{\omega_c\left(1 + \dfrac{kTN_A}{2qn_i\phi_s}\right)} \approx \frac{2qn_i\phi_s}{\omega_c kTN_A} \qquad [25]$$

Effect of doping density.—The effect of doping density on surface photovoltage *vs.* frequency is shown in Fig. 12. In the depletion regime the induced semiconductor surface potential is ϕ_s, determined by the positive surface charge. The scr width, *W*, is given by

$$W = \sqrt{\frac{2K_s\varepsilon_o\phi_s}{qN_A}} \qquad [26]$$

With the scr width inversely proportional to doping density, the corner frequency is reduced as the doping density increases.

Figures 11 and 12 show clearly that frequency-dependent surface photovoltage plots are not straightforward to interpret. The corner frequency, that is used to determine the lifetime, depends on temperature, doping density, and lifetime.

Results

AC-SPV.—The ac photovoltage was measured with the Semiconductor Diagnostics Epi Tau FAast 330 system, using a chemically induced surface scr, not deposited corona charge. We characterized epitaxial wafers with two different doping profiles. The p/p$^+$ sample consists of an epitaxial layer, doped to 10^{15} cm^{-3}, deposited on a highly doped substrate doped to 10^{18} cm^{-3}. The p/p$^-$ sample consists of an epitaxial layer, doped to 10^{15} cm^{-3}, deposited on a moderately doped substrate doped to 10^{15} cm^{-3}. The epitaxial layer thicknesses are 5 μm and 10 μm for both samples. The frequency and temperature dependence of the surface photovoltage and phase of the 10 μm, p/p$^+$ sample is shown in Fig. 13. The agreement between theory and experiment is excellent. The lifetime τ_{scro} had to be changed from 1.3×10^{-6} s at 300 K to 1.6×10^{-6} s at 330 K for theory and experiment to agree, consistent with lifetime increas-

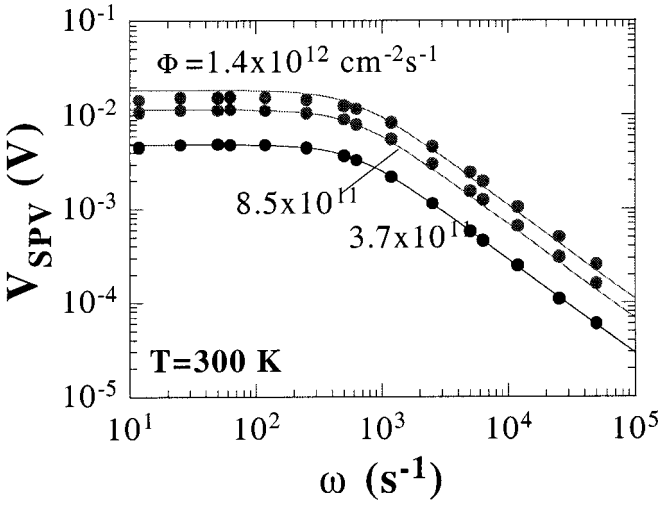

Figure 15. Surface photovoltage *vs.* ω_c for various photon flux densities. $\tau_{scro} = 1$ μs, $\tau_{ro} = 10$ μs, $T = 300$ K, $t_{epi} = 5$ μm, $N_{A,epi} = 10^{15}$ cm^{-3}, $N_{A,sub} = 10^{15}$ cm^{-3}. Points: experiment; lines: theory.

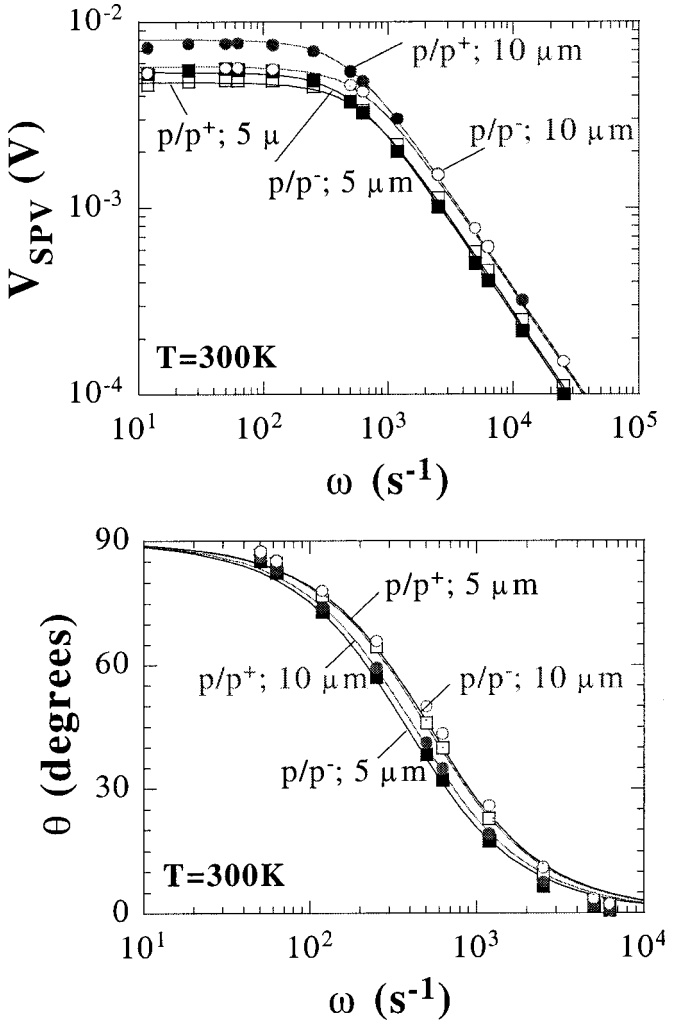

Figure 16. Surface photovoltage and phase angle *vs.* frequency. τ_{scro} :1.0 to 1.3 μs, $\tau_{ro} = 10$ μs, $T = 300$ K. Points: experiment; lines: theory.

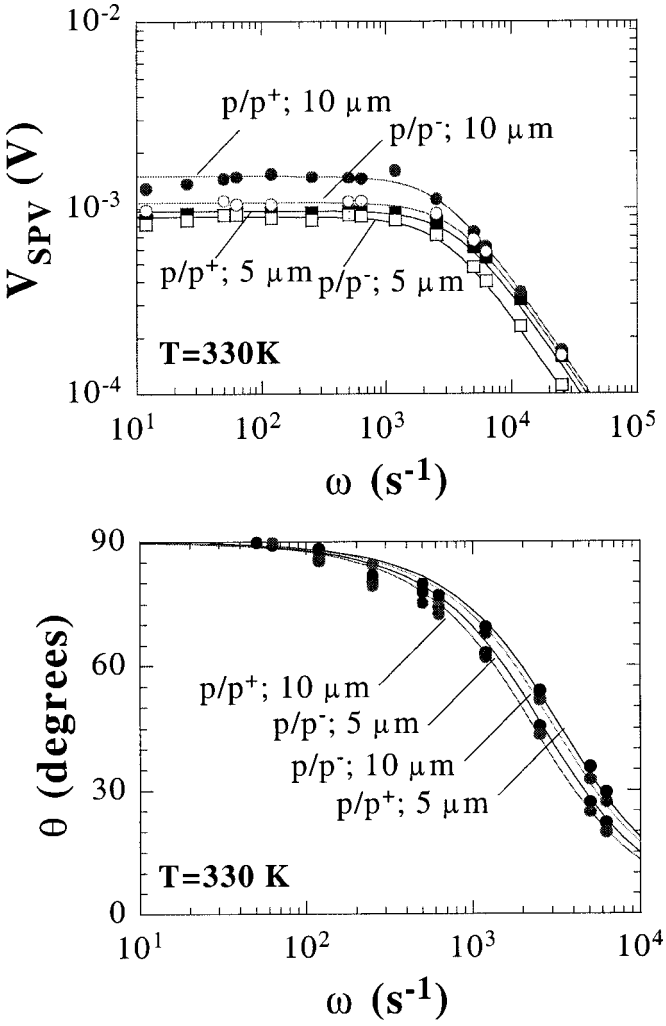

Figure 17. Surface photovoltage and phase angle *vs.* frequency. τ_{scro} :1.2 to 1.6 μs, $\tau_{ro} = 10$ μs, $T = 330$ K. Points: experiment; lines: theory.

ing with increasing temperature in silicon. The Arrhenius plot of the corner frequency in Fig. 14 leads to an activation energy of 0.47 eV.

The effect of photon flux density is shown on Fig. 15. Only the magnitude of the surface photovoltage signals changes without altering the corner frequency. The photon flux density was adjusted experimentally by varying the supply voltage to the laser source. The values shown on Fig. 15 were used for the theory. The ac-SPV method is suitable for bare and oxidized wafers. We find we require a higher photon flux density for oxidized wafers for surface photovoltages of a few tenths to a few mV. The reason for this is not clear. It may be related to surface reflectance.

The effects of substrate doping density and epi layer thickness on V_{SPV} and phase are shown in Fig. 16 and 17. Figure 16 shows experimental data and theoretical curves for 300 K, and Fig. 17 shows data and curves for 330 K. The agreement between experimental data and our theory is excellent in all cases for both surface photovoltage and phase. The space-charge recombination lifetimes and photon flux densities necessary to give this agreement are shown in Table I. Note that in all cases, the lifetime increases with increasing temperature, as expected. The lifetimes of the p/p^+ samples are very similar to those for the p/p^- samples for both thicknesses.

DC-SPV.—To compare the frequency-dependent method with conventional surface photovoltage diffusion length measurements, we measured the diffusion length of both epitaxial wafers

Table I. Sample type, thickness, measurement temperature, near-surface lifetime (measured by the ac technique of this paper), minority carrier diffusion length (measured by conventional SPV), and generation lifetime (measured by pulsed MOS capacitor).

Sample	Thickness (μm)	Temperature (K)	Near-surface lifetime (μs)	Diffusion length (μm)	Generation lifetime (μs)
p/p^+	5	300	1.3	4.5	235
p/p^+	10	300	1.3	7	142
p/p^-	5	300	1.2	330	104
p/p^-	10	300	1.2	304	113
p/p^+	5	330	1.5		
p/p^+	10	330	1.5		
p/p^-	5	330	1.6		
p/p^-	10	330	1.6		

(p/p^+:$10^{15}/10^{18}$ cm^{-3}; p/p^-:$10^{15}/10^{15}$ cm^{-3}). In these measurements, photons with low absorption coefficients are used leading to carrier excitation through the epitaxial layer and a significant portion of the substrate. In that case, it is mainly the thickness of the epitaxial layer that is measured, if the diffusion length of the substrate is significantly lower than that of the p-epi layer, as it would be for the p/p^+ samples.[19] Our results are shown in Table I. For the p/p^+ samples, the diffusion lengths are indeed approximately equal to the layer thicknesses, while for the p/p^- samples there is no relationship with thickness, as expected.

Generation lifetimes.—The method in this paper is an scr-confined recombination lifetime measurement, because excess carriers are created by light. Another scr-confined measurement is the pulsed MOS capacitor technique, in which the device is pulse biased into deep depletion and the recovery time of the device due to thermal electron-hole pair generation is measured leading to the generation lifetime τ_g.[1] We have made such measurements on these wafers, after oxidizing them and forming gates. Generation lifetimes are typically much higher than recombination lifetimes.[20] Table I also shows τ_g with values of several hundred microseconds, much higher than the effective lifetimes of around 1 μs. The higher lifetimes of the p/p^+ wafers may be related to the heavily doped p^+ substrates acting as getters for heavy metals like iron.[21] This gettering effect is not active in the p/p^- wafers.

Discussion

We have developed the theory for optical ac surface photovoltage measurements and verified it with experimental data. We show that when the optically generated carriers are confined to the surface charge-induced scr by using high absorption coefficient photons, the ac surface photovoltage response is governed by recombination in the scr and by surface recombination. We call this lifetime the near-surface lifetime. Recombination in the quasi-neutral region plays a minor role, as does scr and qnr generation. For the samples in this study, the scr recombination lifetime is about 1 μs, a surprisingly low value. This value holds for both p/p^+ and p/p^- wafers with epitaxial layer thicknesses of 5 and 10 μm. Conventional surface photovoltage measurements gave minority carrier diffusion lengths of about the epilayer thickness for the p/p^+ samples and about 300 μm for the p/p^- samples. Generation lifetimes ranged between 100 and 200 μs. None of these values agree with one another, as one would expect for epi layers. Assuming the recombination lifetime or the diffusion length of the epi layer to be much higher than that of the heavily doped substrate, one should not expect any values that are representative of the recombination properties of the epi layer since carrier generation during dc SPV measurements extends from the epi layer into the substrate. Only scr confined measurements yield information about the epitaxial film. Such measurements are most commonly made through reverse-biased p-n junction leakage current or pulsed MOS capacitor measurements. The method discussed here, adds an additional option to such measurement. It is attractive because it is contactless using optical excitation, but this near-surface lifetime is strongly influenced by surface recombination.

Conclusions

We have developed the theory to interpret ac surface photovoltage data measured in the frequency domain. The frequency-dependent behavior is a function of the surface potential, the intrinsic and doping densities, space-charge region recombination and surface lifetimes, and temperature. The corner frequency of surface photovoltage *vs*. frequency plots, provides the effective scr recombination lifetime or near-surface lifetime with no appreciable contribution from the quasi-neutral region or the substrate. Our theory and experiments show the ac surface photovoltage to be poorly suited for epitaxial layer characterization, because the results are strongly influenced by surface recombination.

Acknowledgments

The research leading to this paper was partially funded by the Silicon Wafer Engineering and Defect Science Consortium (SiWEDS) (Intel, Komatsu Electronic Metals, MEMC Electronic Materials, Mitsubishi Silicon, Okmetic, Nippon Steel, SEH America, Sumitomo Sitix Silicon, Texas Instruments, and Wacker Siltronic Corp.). We thank P. Edelman and D. Marinskiy from Semiconductor Diagnostics Inc. for illuminating discussions.

Arizona State University assisted in meeting the publication costs of this article.

References

1. D. K. Schroder, *Semiconductor Material and Device Characterization*, 2nd ed., Wiley-Interscience, New York (1998).
2. T. Pavelka and Z. Batari, in *Analytical and Diagnostic Techniques for Semiconductor Materials, Devices, and Processes*, B. O. Kolbesen, C. Claeys, P. Stallhofer. F. Tardiff, J. Benton, T. Shaffner, D. Schroder, S. Kishino, and P. Rai-Choudhury, Editors, PV 99-16, p. 48, The Electrochemical Society Proceedings Series, Pennington, NJ (1999).
3. T. Hara, F. Tamura, and T. Kitamura, *J. Electrochem. Soc.*, **144**, L54 (1997).
4. Y. I. Ogita, N. Tate, H. Masumura, M. Miyazaki, and K. Yakushiji, in *Recombination Lifetime Measurements in Silicon*, D. C. Gupta, F. R. Bacher, and W. M. Hughes, Editors, ASTM STP 1340, p. 168, Philadelphia, PA (1998).
5. C. Claeys, E. Simoen, A. Poyai, and A. Czerwinski, *J. Electrochem. Soc.*, **146**, 3429 (1999).
6. S. Y. Lee and D. K. Schroder, *Solid-State Electron.*, **43**, 103 (1999).
7. D. K. Schroder, J. E. Park, S. E. Tan, B. D. Choi, S. Kishino, and H. Yoshida, *IEEE Trans. Electron Devices*, **47**, 1653 (2000).
8. R. S. Nakhmanson, *Solid-State Electron.*, **18**, 617 (1975); R. S. Nakhmanson, *Solid-State Electron.*, **18**, 627 (1975).
9. D. K. Schroder, M. S. Fung, R. L. Verkuil, S. Pandey, W. H. Howland, and M. Kleefstra, *Solid-State Electron.*, **42**, 505 (1998).
10. Y. Murakami, H. Abe, and T. Shingyouji, *Jpn. J. Appl. Phys.*, **34**, 1477 (1995).
11. E. Kamieniecki, in *Recombination Lifetime Measurements in Silicon*, D. C. Gupta, F. R. Bacher, and W. M. Hughes, Editors, ASTM STP 1340, p. 147, Philadelphia, PA (1998).
12. *Contamination Monitoring System Based on SPV Diffusion Length Measurements*, Semiconductor Diagnostics, Inc. Manual (1993).
13. R. B. Comizzoli, *J. Electrochem. Soc.*, **134**, 424 (1987).
14. P. Renaud and A. Walker, *Solid State Technol.*, **43**, 143 (2000).
15. Lord Kelvin, *Philos. Mag.*, **46**, 82 (1898).
16. L. Kronik and Y. Shapira, *Surf. Sci. Rep.*, **37**, 1 (1999).
17. E. O. Johnson, *Phys. Rev.*, **111**, 153 (1958).
18. J. P. McKelvey, *Solid State and Semiconductor Physics*, Harper and Row, New York (1966).
19. J. W. Slotboom and M. J. J. Theunissen, *IEEE Electron Device Lett.*, **EDL-4**, 403 (1983); D. K. Schroder, *Solid-State Electron.*, **27**, 247 (1984); C. W. Pearce and R. J. Jaccodine, *IEEE Trans. Electron Dev.*, **38**, 2155 (1991).
20. D. K. Schroder, *IEEE Trans. Electron Devices*, **ED-29**, 1336 (1982).
21. A. L. Smith, K. Wada, and L. C. Kimerling, *J. Electrochem. Soc.*, **147**, 1154 (2000).